INFECTION AND IMMUNITY, Nov. 1999, p. 6056–6066 Vol. 67, No. 11
0019-9567/99/$04.00+0

Increased Interleukin-1 (IL-1) and Imbalance between IL-1 and IL-1 Receptor Antagonist during Acute Inflammation in Experimental Shigellosis

JOSETTE ARONDEL,[1] MONIQUE SINGER,[2] AKIHIRO MATSUKAWA,[3] ARTURO ZYCHLINSKY,[4] AND PHILIPPE J. SANSONETTI[1]*

Unité de Pathogénie Microbienne Moléculaire/Unité INSERM 389[1] and Unité de Pharmacologie Cellulaire/Unité INSERM 485,[2] Institut Pasteur, 75724 Paris Cedex 15, France; Department of Pathology, Kumamoto University Medical School, Kumamoto 860, Japan[3]; and Department of Microbiology, Skirball Institute, New York University Medical Center, New York, New York 10016[4]

Received 24 March 1999/Returned for modification 11 May 1999/Accepted 5 August 1999

Infection by the enteric bacterial pathogen *Shigella* results in intense mucosal inflammation and destruction of the colonic and rectal epithelium in infected humans. Initial bacterial translocation occurs through the follicle-associated epithelium. Previous experiments suggest that interleukin-1 (IL-1) is crucial to trigger inflammation, particularly in the follicular zones. During the first 4 hours of infection in a rabbit ligated-loop model of intestinal invasion, there are two salient characteristics: (i) a high concentration of IL-1α and IL-1β, both in infected Peyer's patch tissue and in the corresponding efferent mesenteric blood, and (ii) a very low level of expression of IL-1 receptor antagonist (IL-1ra). These may reflect a combination of regulation of expression and secretion of IL-1α, IL-1β, and IL-1ra by both resident and recruited phagocytes and the induction of mononuclear phagocyte apoptosis by *Shigella*. This low IL-1ra/IL-1 ratio likely accounts for the rapid, uncontrolled inflammation characteristic of shigellosis.

Shigellosis is an acute inflammatory disease of the colonic and rectal mucosae in humans. In its major form, mucosal tissue destruction generated by acute inflammation causes the dysenteric symptoms characterized by bloody, mucopurulent stools. *Shigella*, the causative agent, invades the colonic and rectal mucosae, particularly epithelial cells (37). *Shigella* is a gram-negative bacterium belonging to the family *Enterobacteriaceae*. Acute inflammation following an infection, essentially by recruitment and activation of cells of the innate immune system, such as monocytes and polymorphonuclear leukocytes (PMN), is the cost of rapid eradication of the invading pathogen. The acute inflammation generated by *Shigella* is initially rich in PMN. In shigellosis, inflammation has the paradoxical effect of causing severe damage to the mucosa and allowing further bacterial invasion before the inflammatory response controls the infection (47, 48, 55). Full-blown shigellosis is characterized by severe diffuse intestinal inflammation extending beyond areas of mucosal invasion (27) and by complications reflecting uncontrolled local and systemic inflammation, such as toxic megacolon, colonic perforations, pseudoleukemoid syndrome, and the hemolytic-uremic syndrome (27).

A balance must be maintained in intestinal tissues between inductive and inhibitory signals of inflammation in order to provide protection from the bacterial products released by the commensal flora and to allow proper conditions for healing and regeneration in case of aggression by a noxious agent or a pathogen. This is illustrated by the occurrence of an acute enterocolitis in interleukin-10 (IL-10), IL-2, and T-cell receptor-knockout mice harboring normal intestinal flora but its absence in their germ-free counterparts (35). Invasive bacterial pathogens such as *Shigella*, which cause acute intestinal inflammation, have probably evolved strategies to up-regulate proinflammatory signals and down-regulate anti-inflammatory signals. The gut inflammation observed in shigellosis resembles other infectious and noninfectious colites, such as idiopathic inflammatory bowel diseases (IBD). Moreover, the histopathological lesions of shigellosis are similar to those of acute-stage ulcerative colitis.

Initial translocation of *Shigella* through the epithelial barrier occurs via M cells of the follicle-associated epithelium (FAE) (53, 56, 59). This makes colonic and rectal lymphoid solitary nodules and their associated dome the major site of initial inflammation, which may then extend, due to the capacity of *Shigella* to enter cells at their basolateral poles (46) and to spread from cell to cell (8).

Upon contact with target cells, *Shigella* secretes four invasion plasmid antigens (Ipa proteins) via a type III secretory apparatus called Mxi-Spa (42–44). In the presence of epithelial cells, Ipa proteins induce major cytoskeletal rearrangements which mediate bacterial entry via macropinocytosis (1). The bacteria then spread from cell to cell via an actin-dependent process involving IcsA, a protein polarly exposed at the bacterial surface, which nucleates and amplifies actin polymerization (8, 23, 39). In the presence of macrophages, IpaB causes rapid apoptotic death of these cells both in vitro (12, 64, 67) and in vivo (33, 66).

When macrophages are preactivated with lipopolysaccharide (LPS) and subsequently infected by invasive *Shigella flexneri*, they release large quantities of mature IL-1β (65). This reflects direct activation of ICE (caspase 1) by IpaB in infected macrophages (12, 31). *Shigella* is therefore able to achieve a dual function (63) in a single cell population: cell killing, which may protect the invasive microorganism against rapid eradication by phagocytic cells in subepithelial tissues, and initiation of early inflammation mediated by IL-1β.

We have previously shown that by initiating inflammation, IL-1 accounts for a rupture of the epithelial barrier that en-

* Corresponding author. Mailing address: Unité de Pathogénie Microbienne Moléculaire/Unité INSERM 389, Institut Pasteur, 25-28 Rue du Docteur Roux, 75724 Paris Cedex 15, France. Phone: (33) (0)1 45 68 83 42. Fax: (33) (0)1 45 68 89 53. E-mail: psanson@pasteur.fr.

hances bacterial invasion (47, 48) and initiates a cascade leading to tissue destruction. Treatment of infected rabbits with IL-1 receptor antagonist (IL-1ra) can significantly reverse both effects (55). Here we show that in the course of experimental shigellosis in the rabbit ligated-loop infection model, the balance between IL-1ra and IL-1 expression in infected follicular structures is severely impaired at the early stage of bacterial invasion, possibly due to macrophage apoptosis. Insufficient expression of IL-1ra may largely account for the severity of inflammation.

MATERIALS AND METHODS

Bacterial strains and culture conditions. M90T is a wild-type *S. flexneri* serotype 5 strain (54). BS15 is a noninvasive derivative of M90T which was cured of the 220-kb plasmid pWR100 and transformed with the recombinant plasmid pRKB15 (66) encoding AFR1, an adherence pilus of the rabbit-specific *Escherichia coli* strain RDEC-1 (13). Prior to experimental infection of rabbits, the bacteria were streaked on Congo red agar. Congo red-positive colonies were resuspended in tryptic soy broth (Diagnostics Pasteur, Marnes la Coquette, France), plated on tryptic soy agar plates, and cultured overnight to confluency at 37°C. The bacteria were harvested in sterile 0.9% NaCl, and their concentration was adjusted to 10^{10} bacteria per ml.

Experimental *Shigella* infection of rabbits. A total of 24 specific-pathogen-free male New Zealand White rabbits, weighing between 2.5 and 3 kg (CEGAV S.S.C., Les Hautes Noës, France), were used in this study. Twelve animals were infected with M90T, and 12 animals were infected with BS15. In each group, four animals were sacrificed 2, 4, or 8 h postinfection. The rabbits received general anesthesia combining acepromazine (250 mg/kg of body weight) (Calmivet, Magny-Vernois, France) intravenously (i.v.) and ketamine (20 mg/kg) (Rhône Mérieux, Lyon, France) i.v. After a laparotomy, ligated loops 5 cm long were made, each containing a Peyer's patch. Depending on the number of Peyer's patches available, between five and six loops were made in each rabbit. Ligations were carefully performed to preserve the afferent and efferent mesenteric vasculature. Inocula of 5×10^9 bacteria in 0.5 ml were injected in each loop. The abdominal cavity was then closed. Two, 4, and 8 h postinfection, the rabbits were again anesthetized with ketamine (20 mg/kg) and laparotomized. The mesenteric vein draining each infected loop was sampled with a 26-gauge by 1/2-in. needle mounted on a 1-ml syringe, and 50 to 100 μl of blood was aspirated and immediately mixed with an anticoagulant and a cocktail of protease inhibitors (0.05% [wt/vol] sodium azide, 1 mg of aprotinin/ml, 1 mg of leupeptin/ml, 1 mg of pepstatin A/ml, and 1 mM AEBSF [all components from Sigma]). Plasma was collected after centrifugation and conserved at −80°C. The animals were then sacrificed by i.v. injection of a 10-ml air bolus. The loops were quickly dissected and opened, and sections of the Peyer's patches were sampled with a skin biopsy punch providing disks 8 mm in diameter (Stiefel, Nanterre, France). The biopsy material was immediately cut into two equal pieces. One half was frozen in liquid nitrogen and stored at −80°C for further extraction of mRNA. The other half was put in 2 ml of cold phosphate-buffered saline (PBS) containing a cocktail of protease inhibitors (see above) and homogenized in ice for 10 s with an Ultra-Turrax homogenizer (Janke & Kunkel GmbH, Staufen, Germany). The samples were then centrifuged at 100,000 × *g* for 1 h at 15°C, and the supernatants were immediately stored at −80°C for cytokine quantification.

Bacterial counts in tissue samples. Peyer's patches from animals infected for 2, 4, or 8 h were punched with a skin biopsy device, providing a disk 6 mm in diameter. The biopsied tissue samples were immersed in a gentamicin solution and washed extensively in cold 0.1× PBS. Tissue samples were then ground with an Ultra-Turrax apparatus and resuspended in a final volume of 1 ml. Dilutions were spread on tryptic soy agar plates after a 30-min incubation at 37°C. Colonies were counted, and CFU were calculated for 1 ml of tissue homogenate.

Immunohistochemistry. Tissues were fixed in 4% formalin, dehydrated, and embedded in historesin (Leica Instruments, Heidelberg, Germany). Blocks were sectioned in 5-μm-thick slices. Immunostaining of the sections was performed with the following antibodies: LPS was labeled by using a biotinylated mouse monoclonal antibody (immunoglobulin G3, kappa chain) directed against the *S. flexneri* serotype 5 somatic antigen (49). IL-1α, IL-1β, and IL-1ra were labeled by their respective specific monoclonal antibodies, which will be identified below. A RAM11-specific monoclonal antibody (Dako Corporation, Carpinteria, Calif.) was used to detect the macrophage population expressing this molecule. In order to label the primary antibody, the LSAB Kit-Peroxidase (Dako Corporation) was used. Briefly, the technique is based on the streptavidin biotin reaction. Endogenous peroxidase activity is quenched by first incubating the samples in 3% H_2O_2 for 5 min. The samples are then incubated with the primary antibody, followed by sequential 10-min incubations with biotinylated antibody and peroxidase-labeled streptavidin. Amplification is obtained by 30-min incubation with the ABC peroxidase kit (Vectastain ABC; Vector Laboratories, Inc., Burlingame, Calif.). Staining is obtained by a 10-min incubation with the freshly prepared substrate chromogen (DAB) solution (3,3′-diaminobenzidine tetrahydrochloride–H_2O_2 [Dako]). Counterstaining is obtained with Harris hematoxylin (Merck, Rahway, N.J.). Final mounting is done on Glycerogel (Dako).

In situ detection of fragmented DNA. Terminal deoxynucleotidyltransferase-mediated dUTP-biotin nick end labeling (TUNEL) was performed as described by Gavrieli et al. (22). Deparaffinized tissue sections were sequentially treated with acetone and proteinase K (Boehringer Mannheim, Indianapolis, Ind.). Labeling was done with the apoptosis detection system fluorescein kit (Promega, Madison, Wis.). Each field was scanned with a confocal microscope (Leica) in both channels. The sections were reconstructed with Adobe Photoshop.

Quantification of IL-1β and IL-1ra. Stored plasmas and supernatants of Peyer's patch homogenates were tested in a sandwich enzyme-linked immunosorbent assay employing antibodies specific for rabbit IL-1β and IL-1ra as described previously (41). Briefly, the wells of microtiter plates were coated with Na carbonate buffer (pH 9.6) with either a mouse monoclonal immunoglobulin G directed against IL-1ra or a sheep polyclonal serum directed against both pro- and mature rabbit IL-1β. After being washed with PBS-Tween 20 (0.05%) and saturated with PBS-bovine serum albumin (1%), plaques were incubated overnight at 4°C with 100 μl of sample. They were washed again before anti-IL-1β or anti-IL-1ra biotinylated antibodies were added at a concentration of 5 μg/ml; the reaction was amplified by 100 μl of the avidin-biotin peroxidase complex (Vectastain; Vector Laboratories). After being washed, the enzyme-linked immunosorbent assay reaction was revealed by the addition of 100 μl of citrate buffer (pH 5.6) containing 0.3 mg of *O*-phenylenediamine/ml and 0.03% H_2O_2. The reaction was stopped by the addition of 4 N H_2SO_4. Optical density was read at 490 nm. Controls were run in parallel on each plaque with a series of dilutions from 1 to 3,000 pg/100 μl of IL-1β and IL-1ra.

IL-1α quantification by RIA. IL-1α concentrations were determined by a radioimmunoassay (RIA) technique based on the competition for a sheep antiserum against rabbit IL-1α between cold IL-1α contained in the samples and a recombinant rabbit IL-1α labeled with ^{125}I (the kit for RIA was from Endogen, Cambridge, Mass.). A second antibody was used to immunoprecipitate the first antibody binding to labeled or cold IL-1α. Radioactivity was read in a gamma counter (Beckman, Palo Alto, Calif.) and compared to a standard curve.

Titration of mRNA for IL-1α, IL-1β, and IL-1ra by RT-PCR in tissues. Total RNA was extracted from 100 mg of frozen Peyer's patch tissue with guanidine thiocyanate (Bioprobe Systems, Montreuil sous Bois, France) as previously described (14) and according to the manufacturer's instructions. Reverse transcription (RT)-PCR was performed with specific primers which are detailed in Table 1.

For rabbit IL-1α (21), primers were designed on two different exons, based on sequence alignments between IL-1α and IL-1β (GenBank accession no. M26295) obtained on Clustal V multiple sequence alignment (61) and with the PCRare program (25). The cDNAs were synthesized after RQ_1Dnase treatment (2U; Promega France, Charbonnières, France) in a total volume of 50 μl, using 10 μg of total RNAs and 0.5 μg of oligo$(dT)_{12–18}$ (Promega France) as a primer, 1.25 mM deoxynucleoside triphosphate, 0.5 U of RNasin (Promega France), and 200 U of Moloney murine leukemia virus reverse transcriptase RNase-H minus (Promega France) in the manufacturer's buffer for 1 h at 42°C. PCRs were performed on a PHc-2 (Techne Inc., Rahway, N.J.). For a 100-μl reaction mixture, 5 μl of cDNA (serial dilutions), primers (1 μM each), deoxynucleoside triphosphates (0.2 mM each), $MgCl_2$ (1.5 to 3 mM), and Eurobiotaq DNA polymerase (3.5 U; Eurobio, Les Ulis, France) in the manufacturer's buffer were used. The thermocycling protocol was as follows: 95°C for 3 min, then *x* cycles (Table 1) of denaturation at 94°C for 45 s, hybridization at annealing temperature (Table 1) for 1.5 min, elongation at 72°C for 1.5 min, and a final incubation at 72°C for 7 min. The amplification products were resolved on a 1.5% agarose gel containing 0.5 μg of ethidium bromide/ml and then transferred to a nylon membrane (Hybond N^+; Amersham, Courtaboeuf, France) in 0.4 N NaOH and hybridized overnight at 60°C with the corresponding oligonucleotide probes (Table 1) in Denhardt's reagent. The oligonucleotides (5 pmol) were 5′ end labeled with T4 polynucleotide kinase (3 U; Pharmacia, Orsay, France) with 30 μCi of [γ-^{32}P]ATP (5,000 Ci/mmol; Amersham) for 1 h at 37°C. Washing was performed two times for 30 min each time in 2× saline sodium citrate–0.1% sodium dodecyl sulfate and two times for 30 min each time in 0.5× SSC (1× SSC is 0.15 M NaCl plus 0.015 M sodium citrate), and semiquantive analysis was achieved on a PhosphorImager (Molecular Dynamics, Sunnyvale, Calif.), using Image Quant, comparing target molecule levels to γ-actin levels. We ensured that measurements were performed in the exponential phase of the reaction by varying cDNA dilutions and cycle number.

Statistical analysis. We used the nonparametric Mann-Whitney test (rank-sum test) for determination of the statistical significance of differences between mean values. A probability of ≤0.05 defined this significance.

RESULTS

Rabbits were laparotomized, and intestinal loops containing a Peyer's patch were ligated and injected either with the *S. flexneri* wild-type strain, M90T, or with the control strain, BS15, or with sterile saline. BS15 is a derivative of M90T in which the virulence plasmid pWR100 was cured and the strain was transfected with plasmid pRKB15 encoding AFR1, an adherence pilus of the rabbit-specific enteropathogenic *E. coli* strain

TABLE 1. Primers used in RT-PCR

Molecule	Oligonucleotide	Temp (°C)	Maximal no. of cycles	PCR product size (bp)	Reference
IL-1α	Sense: CCACTACAAAATCTGGGCGATGCA Antisense: CAGAAGAAGAGGATGTCACTCCTCG Probe: TATACTTCCTGTAACTTTAAGAATCTC	66	33	213	21
IL-1β	Sense: AAAGCAGTTCCCTGCCCACAGGCC Antisense: TGGGTAACGGTTGGGGTCTACACT Probe: TGCAACACCTGGGATGACTACAGTCTTGAG	66	30	388	10
icIL-1ra	Sense: GGACTCCACACAACCCACAAGACC Antisense: CTACTGGTCCTCCTGGAAGTAGAA Probe: GACCCTCCCTATGGCTTCAGA	64	35	511	40
sIL-1ra	Sense: GAAGGTCTTCTGGTTAACATCCCA Antisense: ATGAGACCCTCCAGGAGCACCCGC Probe: AGGCACCTAATCTCCCTCCTCCTC	64	35	150	40
γ-Actin	Sense: CCATCGTGGGGCGTCCGCGGCA Antisense: ATCTGGGTCATCTTCTCGCGGT Probe: GCGACGAGGCCCAGAGCAAGCGTG	62	26	268	28

RDEC-1 (13). AFR1 directs RDEC-1 primarily to M cells of the FAE and allows translocation of these bacteria to Peyer's patches (32). AFR1 allows translocation of BS15 through the FAE in a quantity similar to that of its invasive counterpart (56, 66). The tissue lesions observed in the present study were similar in their time of occurrence, quantity, and quality to those described in previous contributions, particularly one in which the M90T and BS15 strains were studied in parallel (56).

Infections with M90T and BS15 resulted in levels of bacterial invasion of Peyer's patches similar to those already shown (66), due to the AFR1 adhesin allowing a translocation efficiency through the FAE comparable to that caused by expression of the *Shigella* invasive phenotype. Two hours after infection, there were $(2.1 \pm 1.4) \times 10^4$ CFU/ml (mean ± standard deviation) in Peyer's patches infected with M90T and $(2.8 \pm 0.9) \times 10^4$ CFU/ml in infection with BS15. Four hours after infection, the numbers of CFU were $(5.3 \pm 1.9) \times 10^4$/ml for M90T and $(6.2 \pm 2.1) \times 10^4$/ml for BS15. Eight hours after infection, the numbers of CFU were $(13.7 \pm 5.8) \times 10^5$/ml for M90T and $(15.6 \pm 4.2) \times 10^4$ CFU/ml for BS15.

Blood from the mesenteric vein and Peyer's patch tissues was sampled 2, 4, and 8 h postinfection. IL-1α, IL-1β, and IL-1ra were measured as described in Materials and Methods.

Concentration of IL-1α and IL-1β in plasma and Peyer's patch tissue. As shown in Fig. 1A, the concentrations of IL-1α in plasma increased during the time course of infection and were significantly higher in animals infected with M90T at 2, 4, and 8 h after infection (1.08, 2.25 ± 0.45, and 2.65 ± 0.5 ng/ml, respectively) than in animals infected with BS15 (0.04 ± 0.04, 0.13, and 0.92 ± 0.1 ng/ml, respectively). As shown in Fig. 1B, consistent results were obtained with tissue samples in which, at the three time periods, IL-1α concentrations were higher in animals infected with M90T (0.86 ± 0.1, 3.48 ± 0.7, and 3.63 ± 0.7 ng/ml, respectively) than in animals infected with BS15 (0.04 ± 0.04, 1.53 ± 0.1, and 1.8 ± 0.18 ng/ml, respectively). In both plasma and tissue samples, comparison of mean IL-1α concentrations at a given time point in intestinal loops infected with M90T or BS15 showed a P value of ≤ 0.05, thus confirming the statistical significance. This series of results demonstrated that the invasive strain M90T had the capacity, at each time point, to induce higher IL-1α production than its noninvasive-adhesive counterpart.

Similarly, as shown in Fig. 1C, concentrations of IL-1β in plasma samples were consistently higher in animals infected with M90T at 2, 4, and 8 h after infection (0.15 ± 0.15, 0.13 ± 0.01, and 0.23 ± 0.1 ng/ml, respectively) than in animals infected with BS15 (0.06 ± 0.01, 0.11, and 0.07 ± 0.01 ng/ml, respectively). However, only the samples taken at 8 h showed a statistically significant difference between M90T- and BS15-infected loops, with a P value of <0.05. Consistent results, shown in Fig. 1D, were obtained from tissue samples in which, at the three time periods, IL-1β concentrations were higher in animals infected with M90T (1.65 ± 0.5, 4.18 ± 1.7, and 7.5 ± 1.7 ng/ml, respectively) than in animals infected with BS15 (0.62 ± 0.2, 2.04 ± 0.8, and 1.53 ± 0.4 ng/ml, respectively). At the three time points, differences in mean IL-1β concentrations between intestinal loops infected with M90T or BS15 appeared statistically significant, with a P value of <0.05.

In the Peyer's patch tissue samples of control intestinal loops infected with saline, levels of both IL-1α and IL-1β were stable and very low at 2, 4, and 8 h compared to those corresponding to infected tissues. After 8 h, the mean control values of tissue IL-1α and IL-1β were 0.58 ± 0.10 and 0.69 ± 0.22 ng/ml of tissue suspension, respectively.

Taken together, these results demonstrate the rapid and specific release of IL-1α and IL-1β, first to lymphoid tissue and eventually into circulation.

Concentration of IL-1ra in plasma and Peyer's patches. As shown in Fig. 1E, the concentration of IL-1ra in plasma samples was significantly lower after 2 and 4 h of infection in animals infected with M90T (1.26 ± 0.43 and 1.62 ± 0.57 ng/ml, respectively) than in animals infected by BS15 (4.97 ± 1.38 and 45.43 ± 12 ng/ml, respectively). At these two time points, differences in mean IL-1ra concentrations between loops infected with M90T or BS15 appeared statistically significant, with a P value of <0.05. After 8 h of infection, however, plasma and tissue concentrations of IL-1ra in M90T-infected loops had risen and even surpassed those measured in animals infected with BS15, in which IL-1ra concentrations had consistently decreased (13.68 ± 3.9 and 2.82 ng/ml, respectively). Similar trends were observed in tissue samples, as shown in Fig. 1F. After 2 and 4 h of infection, concentrations of IL-1ra were significantly lower in animals infected with M90T (82.5 ± 20 and 45.3 ± 11 ng/ml, respectively) than in

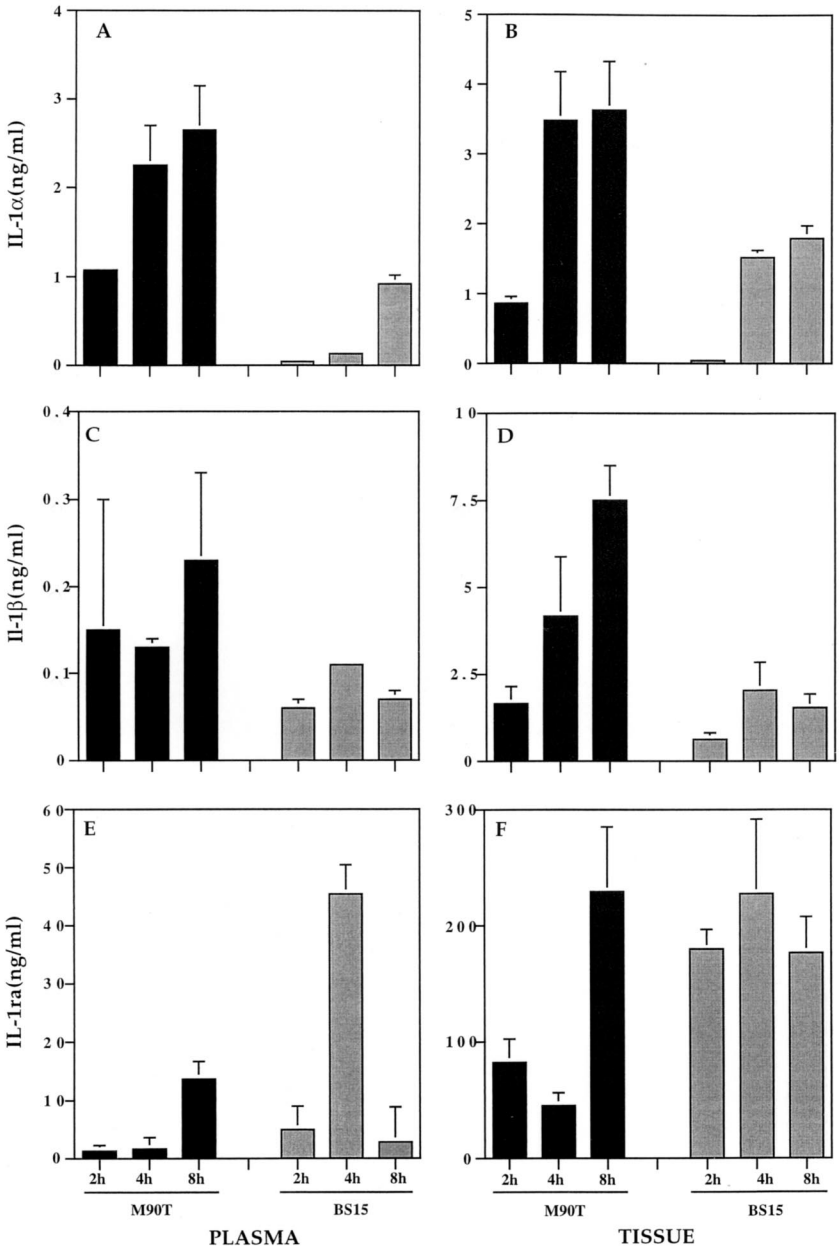

FIG. 1. Shown are IL-1α levels in plasma (A) and in Peyer's patch tissue (B), IL-1β levels in plasma (C) and in Peyer's patch tissue (D), and IL-1ra levels in plasma (E) and in Peyer's patch tissue (F). Cytokine measurements were performed after 2, 4, and 8 h of infection either by invasive *S. flexneri* M90T (solid bars) or by its noninvasive-adhesive derivative, BS15 (shaded bars). The plasma was from blood samples taken from the mesenteric vein draining the infected loop containing the Peyer's patch. The data represent means plus standard deviations.

animals infected with BS15 (179.8 ± 17.1 and 227.6 ± 64 ng/ml, respectively). At these two time points, differences in mean IL-1ra concentrations between loops infected with M90T or BS15 appeared statistically significant, with a P value of <0.05. Similarly, after 8 h of infection, IL-1ra concentrations had risen in M90T-infected samples and had reached concentrations even higher than those observed in BS15-infected tissues (229.22 ± 64 and 176.83 ± 30.7 ng/ml, respectively). This series of results shows a poor IL-1ra response in M90T-infected tissues compared to that in BS15-infected tissues during the first 4 h of infection. By 8 h, however, M90T-infected tissues had compensated for the differences and reached even higher concentrations of IL-1ra. In the Peyer's patch tissue samples from control intestinal loops infected with saline, levels of IL-1ra remained stable according to time. After 8 h, the mean value was 82.5 ± 18.8 ng/ml of tissue suspension.

Balance between IL-1ra and IL-1 in plasma and Peyer's patch tissue. Since IL-1α and IL-1β are proinflammatory and IL-1ra is anti-inflammatory, we calculated the IL-1ra/IL-1 ratio for animals infected with M90T or BS15 at 2, 4, and 8 h postinfection in both plasma and tissue. Thus, high IL-1ra/IL-1 ratios would indicate inhibition of inflammation whereas low IL-1ra/IL-1 ratios are likely to mean a strong inflammation.

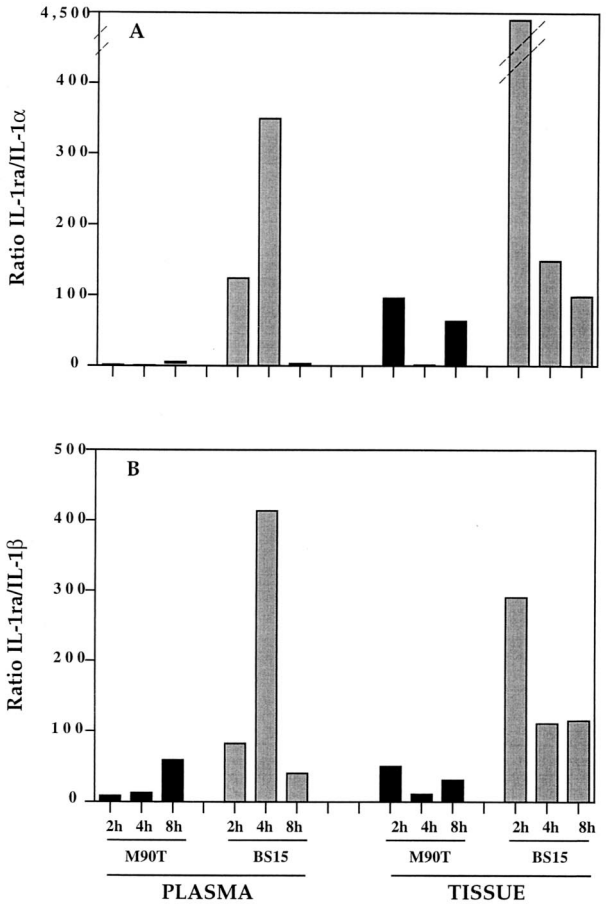

FIG. 2. IL-1ra/IL-1α (A) and IL-1ra/IL-1β (B) ratios in plasma and Peyer's patch tissue during infection with M90T (solid bars) or BS15 (shaded bars).

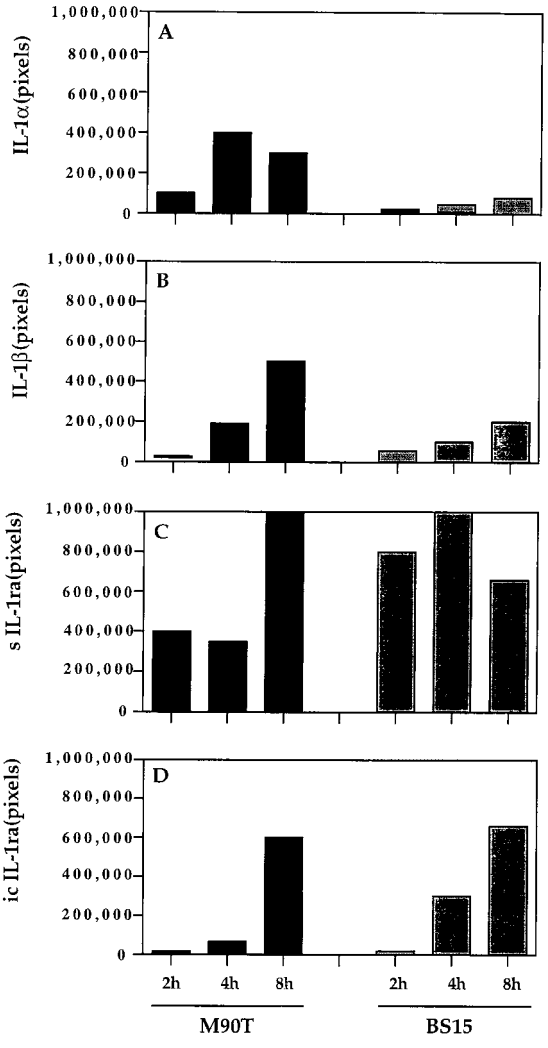

FIG. 3. Semiquantitative measurement of IL-1α, IL-1β, sIL-1ra, and icIL-1ra products of RT-PCR carried out on Peyer's patch tissue samples after 2, 4, and 8 h of infection with either M90T or BS15. The results are representative of the data obtained with four to six Peyer's patches for each time point. The data have been normalized according to the amplification of the γ-actin reverse-transcribed products that were standardized at 500,000 pixels.

The results shown in Fig. 2 indicate a dramatic difference between these ratios, depending on the infecting strain.

The IL-1ra/IL-1β ratio (Fig. 2B), in both plasma and tissues, is much lower in animals infected with M90T after 2 and 4 h of infection than in animals infected with BS15. The most striking difference was observed after 4 h of infection, when the ratio was 34-fold lower in plasma samples and 10-fold lower in tissue samples when M90T was the infecting agent. After 8 h of infection, the ratios tended to equalize.

The difference between M90T and BS15 in the IL-1ra/IL-1α ratio was even more striking (Fig. 2A). Two hours after infection, the ratios were 12- and 47-fold lower in plasma and tissue samples, respectively, when animals were infected with M90T. Four hours postinfection, the ratios were 498- and 121-fold lower in plasma and tissue samples, respectively. Here we also observed a trend toward equalization after 8 h of infection.

In the Peyer's patch tissue samples of control intestinal loops infected with saline, the IL-1ra/IL-1 ratios remained stable. After 8 h, the IL-1ra/IL-1α ratio was 142 and the IL-1ra/IL-1β ratio was 119.

These results indicate that at the early stage of *Shigella* infection (i.e., after 2 and 4 h), M90T caused significantly higher production of IL-1α and IL-1β than did BS15, as well as a major imbalance in the IL-1ra/IL-1 ratio. Thus, the tissues are unable to increase the IL-1ra concentration to a level that would counterbalance the increased IL-1.

Transcription of IL-1ra, IL-1α, and IL-1β mRNAs. We analyzed the level of mRNA for IL-1ra, IL-1α, and IL-1β to determine whether there was transcriptional regulation during the course of an infection by M90T or BS15. RT-PCR was used to analyze the IL-1 and IL-1ra mRNAs. Figure 3 shows the amount of mRNA for IL-1α (A), IL-1β (B), secreted IL-1ra (sIL-1ra) (C), and intracellular IL-1ra (icIL-1ra) (D). The results are reported as the mean values of the numbers of pixels corresponding to hybridization intensities as measured by the phosphorimager. The level of mRNA was normalized to the signal given by γ-actin mRNA, which in these experiments was standardized at a value of 500,000 pixels. In agreement with the concentrations of the translated products, Fig. 3A and B show that the mRNA of IL-1α and IL-1β genes steadily increased with the duration of infection by M90T and BS15, although at a significantly lower level at all time points in tissues infected by BS15. Figure 3C and D show that transcriptional activities of the sIL-1ra and icIL-1ra genes were consis-

tently lower after 2 and 4 h of infection in tissues infected by M90T than in those infected by BS15.

Immunostaining of Peyer's patch sections for LPS, macrophages, IL-1α, IL-1β, and IL-1ra. Figure 4 shows immunostainings performed on serial sections of the same block taken from a Peyer's patch collected after 4 h of infection, either with M90T (A to E) or with BS15 (F to J). Immunostaining with an anti-LPS antibody (Fig. 4A) shows that M90T had already infected the FAE. Higher magnification (data not shown) indicated that a large portion of the invading bacteria was associated with M cells or M-cell pockets, as previously reported (56).

Bacteria were also seen in lower numbers deeper in the dome area of the follicle, indicating that infection remained largely restricted to the epithelial lining, either because the inflammatory reaction was so strong that it controlled bacterial invasion at an early stage or because the cells that had phagocytosed M90T (i.e., macrophages and possibly dendritic cells) were either killed or strongly impaired in their capacity to move deeper into the follicle. In agreement with this hypothesis, at the same time point, significant numbers of BS15 bacteria (Fig. 4F) were seen in M-cell pockets of the FAE but also, with similar density, in the dome of the corresponding follicle. This may indicate that these phagocytosed bacteria are eliciting less killing and/or less motility impairment of phagocytes, thereby achieving larger spread in the follicle. Figure 4B shows immunostaining directed against the rabbit-specific macrophage marker RAM11. Massive macrophage recruitment to the dome area is observed, with some of the cells reaching M-cell pockets. This observation suggests that FAE infected by an invasive microorganism recruits mononuclear phagocytes more efficiently, possibly by secreting high concentrations of mononuclear-cell-specific chemokines. There was a significant overlap between bacterial diffusion and macrophage recruitment, but not the strict colocalization observed with BS15, as exemplified in Fig. 4G, which shows macrophages tightly associated with bacteria both in M-cell pockets and in the dome of the Peyer's patch. Figure 4C shows that a large number of IL-1α-producing cells are present in both the FAE and the dome of the Peyer's patch infected with M90T. Most of the positive cells correspond to cells expressing RAM11 in Fig. 4B. Conversely, there are fewer IL-1α-producing cells in BS15 infection, where macrophages are recruited, than in M90T infection (Fig. 4H). A similar observation can be made in Fig. 4D and I with cells producing IL-1β, which is massively expressed and probably released by the mononuclear cells recruited in the course of M90T infection, whereas less of this cytokine is expressed during BS15 infection. The pattern of IL-1β staining is less associated with individual cells than that of IL-1α. In agreement with the concentrations observed in tissues and draining blood, weak labeling of IL-1ra is observed in both the FAE and the dome of the Peyer's patch infected by M90T compared to that in BS15 infection. After 8 h of infection (data not shown), the numbers of IL-1ra-producing cells were approximately equal in tissues infected with M90T or BS15. In addition, epithelial cells, including M cells, showed strong, homogeneous, and diffuse staining for IL-1α and IL-1β (data not shown), indicating that epithelial cells had become major players in the development of inflammation whereas at earlier time points (i.e., 2 and 4 h) most IL-1 production took place in macrophages and recruited monocytes.

Apoptosis in areas of infection and macrophage accumulation. In order to analyze possible reasons for the low expression of IL-1ra and massive release of IL-1α and IL-1β at 4 h after infection, we looked for apoptosis in the areas of bacterial invasion and macrophage accumulation in Peyer's patches infected either by M90T or by BS15. As shown in Fig. 5A and C, the dome area infected by invasive M90T was characterized by the presence of a large number of apoptotic cells, the majority of which were likely macrophages. On the other hand, as shown in Fig. 5B and D, very few apoptotic cells were observed in areas of tissue infected by the noninvasive strain BS15.

DISCUSSION

IL-1 (IL-1α and IL-1β) is a multipotent, primarily inflammatory cytokine which affects almost any cell type and cooperates with other cytokines, chemokines, and a variety of other mediators. IL-1 is predominantly synthesized by activated macrophages but can also be produced by members of the mononuclear phagocyte family, including dendritic cells, and by other cell populations, such as B lymphocytes, NK cells, endothelial cells, and even epithelial cells under particular circumstances, such as bacterial invasion (17, 34). Production of IL-1 is tightly regulated at the level of gene expression, and its activity is controlled by a variety of molecules, including surface receptors, such as IL-1RII, a nonagonist, decoy receptor (57); soluble receptors, such as IL-1sRI and IL-1sRII (6); and IL-1ra, a specific receptor antagonist (5, 7). This 23- to 25-kDa protein, which, like IL-1, is produced by monocytes/macrophages but also by PMN, fibroblasts, and keratinocytes (4), binds to IL-1RI with affinity almost equal to that of IL-1α and IL-1β (19) but does not transmit a signal (18). As a consequence, IL-1ra blocks IL-1 activity both in vitro and in vivo (4).

There are two major forms of the protein, sIL-1ra, which likely corresponds to the above definition of a nonagonist competitor for IL-1RI, particularly as an antagonist of the secreted form of IL-1β, and icIL-1ra, which shows an altered signal peptide. The physiological function of icIL-1ra, however, is unclear (29).

In an increasing number of infectious and noninfectious clinical and experimental situations, data indicate that IL-1ra may be essential for the host defense against excessive, deleterious inflammation (20, 24, 26, 45, 50, 55). In IBD, and particularly in ulcerative colitis, which shares several clinical and histopathological characteristics with shigellosis, a significant imbalance of the IL-1ra/IL-1 ratio, mostly caused by a decrease of IL-1ra concentrations in intestinal tissues, was found at the acute phase of the disease (11). The lowest IL-1ra/IL-1 ratios were observed in the most severe cases. More recently, an increase in IL-1α and IL-1β was demonstrated in biopsy specimens from patients suffering acute cases of Crohn's disease, ulcerative colitis, and other inflammatory diseases of the colon. The IL-1ra/(IL-1α plus IL-1β) ratio was consistently decreased in these situations. In addition, a genetic influence on the intensity of inflammation based on dysregulation of the IL-1ra/IL-1 balance may account for an increase in disease severity (3, 30, 52).

In patients at the acute and convalescent stages of *S. flexneri* and *Shigella dysenteriae* 1 infection, immunohistochemistry of rectal samples shows a pattern of IL-1, IL-4, IL-6, IL-8, tumor necrosis factor alpha, and gamma interferon hyperproduction. Severe disease is associated with increased numbers of IL-1β-, IL-6–tumor necrosis factor alpha, and gamma interferon-producing cells; IL-1 is essentially produced by monocytes/macrophages, unlike IL-6 and IL-8, which are expressed by epithelial cells (51). These data suggest that IL-1 is a key factor in *Shigella*-induced intestinal inflammation. Our previous observation that IL-1ra reduces intestinal inflammation in experimental shigellosis in the rabbit ligated-loop model of *Shigella* infection (55) represents the experimental complement to these clinical observations and confirms the key role of IL-1 in

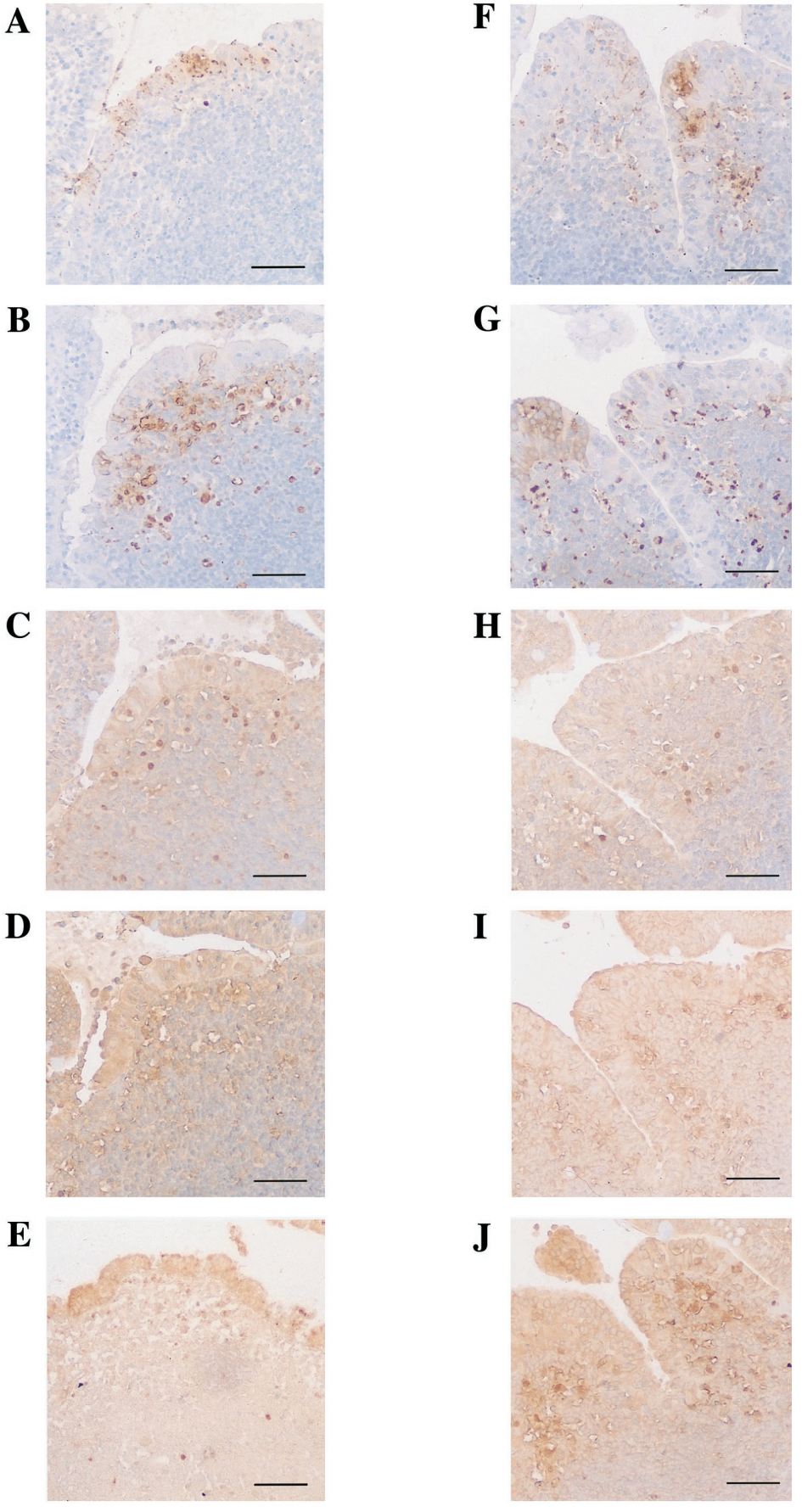

FIG. 4. Immunoperoxidase labeling of Peyer's patch tissue sections after 4 h of infection with M90T (A to E) or BS15 (F to J). The following antigens are labeled: LPS (A and F), RAM11 (a macrophage-specific marker) (B and G), IL-1α (C and H), IL-1β (D and I), and IL-1ra (E and J). Bars = 10 μm.

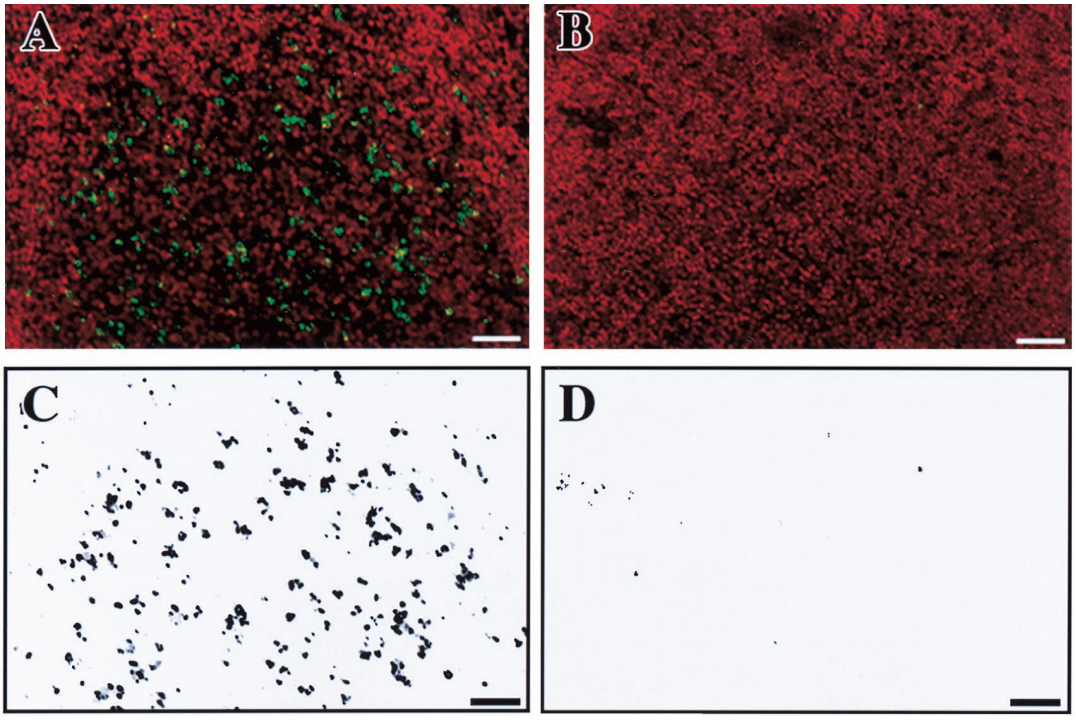

FIG. 5. TUNEL staining of apoptotic cells in the dome area of a lymphoid follicle infected for 4 h either by the invasive isolate, M90T (A), or by the noninvasive-adhesive isolate, BS15 (B). For better evaluation of the density of fluorescein-labeled apoptotic cells in these samples, only the green TUNEL-positive nuclei have been selected and are shown in panel C (derived from panel A) and in panel D (derived from panel B).

the initiation of inflammation. These data also suggest an imbalance in the IL-1ra/IL-1 ratio, as observed in IBD (11). Moreover, in a model of rabbit immune complex colitis, IL-1 gene expression and synthesis occur early (i.e., at 4 h) in the course of experimental disease and levels of IL-1 in tissues, which are in the same order of magnitude as those observed here, correlate with the degree of tissue inflammation, which is reduced by administration of IL-1ra (15, 16).

The aim of this work was to follow the kinetics of IL-1α, IL-1β, and IL-1ra in rabbit ligated loops infected by *S. flexneri*, both in infected tissues and in the mesenteric blood. We followed the balance between these proinflammatory cytokines and their major antagonist during the infection. Infections were carried out in loops containing a Peyer's patch because the FAE that covers Peyer's patches is the major site of *Shigella* invasion of intestinal tissues at early stages of incubation (i.e., at 2 to 4 h); thus, these areas are the major foci of the initiation of inflammation (47, 56, 59). In addition, rapid entry into these areas facilitates synchronization of the infectious process, whereas invasion of villous areas of the intestinal epithelium is delayed and more widespread in time (52a). In addition to invasive M90T, we used a control mutant strain, BS15, a plasmidless, noninvasive mutant of *S. flexneri* M90T which expresses the AFR1 rabbit-specific adherence pilus of the enteropathogenic *E. coli* RDEC-1 (13). This adhesin causes selective binding to the M-cell surface, thus mediating the translocation of bacteria. In consequence, M90T and BS15 reach similar numbers in infected Peyer's patches (56, 66).

The results presented in this paper show an increase in production of IL-1 during progression of the infection. At all time points, tissues infected by the invasive strain M90T contained more IL-1α and IL-1β than those infected with the adhesive-noninvasive strain BS15. Tissue concentrations of IL-1α in Peyer's patches infected by M90T were roughly twofold greater than in those infected by BS15 at all time points, and tissue concentrations of IL-1β were roughly two- to fourfold greater, depending on the time point. This demonstrates that invasive shigellae cause significantly greater release of IL-1 and correlates with the observation that, in spite of its causing significant influx of PMN in the domes of lymphoid follicles after crossing the FAE, BS15 does not induce the extensive inflammatory destruction observed with M90T (56). These results are also in agreement with immunohistochemical observations of human rectal samples (51). Higher production of IL-1α and IL-1β is likely to reflect both higher expression of IL-1 in individual cells and stronger recruitment of these producing cells to the infection site. Accordingly, the number of transcripts for IL-1α and IL-1β followed a trend similar to that measured by the cytokines, as measured by RT-PCR performed on tissue samples. Immunostaining experiments carried out on infected Peyer's patch tissues clearly confirmed the titration experiments; there were higher numbers of IL-1α- and IL-1β-producing cells, as well as a greater amount of these cytokines visible on the tissue sections of Peyer's patches infected with M90T than on those infected with BS15.

Titrations carried out on the plasma obtained from the efferent mesenteric blood samples taken from infected loops were in agreement with these data, showing increasing concentrations of the two cytokines during the infection. Interestingly, however, the ratio of plasma IL-1α to tissue IL-1α was roughly 1 at all time points, whereas the ratio of plasma IL-1β to tissue IL-1β varied between 0.1 and 0.2, thus appearing 10-fold lower. The latter observation was unexpected, because in inflammatory situations, particularly in acute infections, significant levels of circulating IL-1β, but rarely of circulating IL-1α, are observed. This is essentially due to the property of IL-1α of remaining primarily intracellular and being released mostly in situations in which cytosolic leakage can occur, such as in the

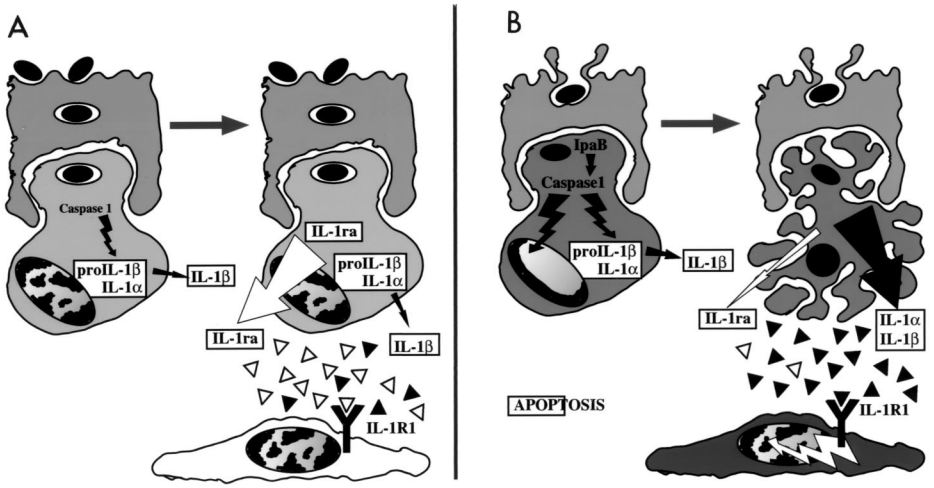

FIG. 6. Scheme summarizing the possible link between macrophage apoptosis in the dome areas of lymphoid follicles infected by a noninvasive (A) or an invasive (B) *Shigella* strain and the imbalance between IL-1 and IL-1ra accounting for severe inflammation observed at the early stage of experimental shigellosis. The top cell is an M cell, and the bottom cell is a macrophage in each panel.

event of cell lysis (58, 60). Conversely, mature IL-1β is normally secreted by activated macrophages following cleavage of the promolecule by caspase 1 (ICE) (9).

Macrophages from ICE knockout mice do not release mature IL-1β in vitro (36, 38). The present observation is likely to reflect a situation of massive killing of preactivated IL-1-producing cells in areas where invading *Shigella* interacts with macrophages, particularly in the domes of follicular structures. This is precisely what was observed here with the early appearance (i.e., at 4 h) of apoptotic cells, likely macrophages, in the apical domes of Peyer's patches infected by M90T. Invasive *Shigella* causes macrophage apoptosis both in vitro (67) and in vivo (66). Apoptotic killing in vivo has been studied under experimental conditions that were similar to those followed in the course of this study. Under such conditions, after 8 h of infection, the number of apoptotic cells is more than 50-fold greater in follicles infected by M90T than in those infected by BS15 (66). IpaB is the major effector of apoptotic death by activating ICE (12). This accounts for early release of mature IL-1β by infected macrophages before they complete their cell death program (31, 65), thereby initiating early inflammation in follicular zones (62, 63). The important extracellular release of IL-1α, which is reflected by its high circulating titer in the mesenteric blood, may be explained by massive killing of resident macrophages and recruited monocytes in the dome area. This profound level of apoptosis overwhelms the phagocytic clearance of apoptotic cells, thus allowing free extracellular IL-1α to be present in tissues and to subsequently pass into the circulation. Based on the above discussion, a model emerges in which not only the difference in transcriptional and translational expression of IL-1α and IL-1β but also the complex intricacy of macrophage activation and macrophage death caused by the invasive phenotype of M90T that makes both forms of IL-1 more readily available to bind IL-1RI and activate the large array of reactive cells present within the invaded zone can account for the difference in induction capacity of tissue inflammation and destruction observed between M90T and BS15.

Surprisingly, in addition to the higher expression of IL-1, M90T also caused a decrease in the expression of IL-1ra in infected tissues at 4 h after infection in comparison with BS15. A twofold and a fivefold decrease were observed at 2 and 4 h, respectively. At 8 h after infection, IL-1ra concentrations caught up, probably due to massive recruitment of producing cells to infected zones. The plasma concentrations reflected the tissue data, with a striking difference observed at 4 h after infection; IL-1ra concentrations were 25-fold lower in mesenteric blood samples corresponding to Peyer's patches infected with M90T than in those infected by BS15. These differences were confirmed when the IL-1ra/IL-1 ratios were calculated. In tissues infected by M90T, IL-1ra/IL-1α and IL-1ra/IL-1β ratios were consistently less than 100, in contrast to tissues infected by BS15, in which those ratios appeared constantly greater and, at 2 h, largely greater than 100.

The major differences appeared at the early 2- and 4-h time points of infection. Ratios in plasma samples dramatically accentuated these differences again at early stages of infection. The levels of mRNA clearly reflected the tissue levels of IL-1ra, with significantly lower activities after 2 and 4 h of infection in tissues infected by M90T than in those infected by BS15. This was observed both for sIL-1ra and icIL-1ra, thereby suggesting a common down-regulatory mechanism. It is possible that killing of macrophages at the early time points of infection accounts for this decrease.

It has previously been shown in human monocytes that LPS has the capacity to induce IL-1 and IL-1ra in the same cell (2). It is therefore possible that after releasing IL-1, the same macrophages and recruited monocytes are unable to compensate for their proinflammatory effect by producing enough IL-1ra because they are apoptotic. After 8 h of infection there is recruitment of PMN and circulating monocytes. Together, these cells control bacterial growth and increase the number of cells that produce IL-1ra, thereby restoring the IL-1ra–IL-1 balance.

It appears, therefore, that the early stage of *Shigella* infection is characterized by an imbalance between IL-1ra and IL-1 whose hypothetical mechanism is summarized in Fig. 6. In addition to the higher level of IL-1 production that characterizes the invasive phenotype, the lack of a proper balance between IL-1ra and IL-1 becomes another key feature of the development of severe inflammation. These studies certainly emphasize the need for experimental systems and analytical tools that would allow us to dissect the very early stages of infectious processes, particularly the early time points of the innate immune response, which are crucial for the development and subsequent healing of the disease lesions.

ACKNOWLEDGMENTS

We thank Dana Philpott for her careful reading of the manuscript and Colette Jacquemin for editing. We also thank Armelle Phalipon and Juana Perdomo for their advice and constant interest in the work.

This work was supported in part by Biotec contract no. 97-C-0227 from the Ministère de l'Enseignement de la Recherche et de la Technologie and NIH grant AI42780.

REFERENCES

1. **Adam, T., M. Arpin, M. C. Prévost, P. Gounon, and P. J. Sansonetti.** 1995. Cytoskeletal rearrangements and the functional role of T-plastin during entry of *Shigella flexneri* into HeLa cells. J. Cell Biol. **129:**367–381.
2. **Andersson, J., L. Björk, C. A. Dinarello, H. Towbin, and U. Andersson.** 1992. Lipopolysaccharide induces human interleukin-1 receptor antagonist and interleukin-1 production in the same cell. Eur. J. Immunol. **22:**2617–2623.
3. **Andus, T., R. Daig, and D. Vogl.** 1997. Imbalance of the interleukin-1 system in colonic mucosa: association with intestinal inflammation and interleukin-1 receptor antagonist genotype 2. Gut **41:**651–657.
4. **Arend, W. P.** 1993. Interleukin-1 receptor antagonist. Adv. Immunol. **54:** 167–227.
5. **Arend, W. P., F. G. Joslin, and R. J. Massoni.** 1985. Effects of immune complexes on production by human monocytes of interleukin 1 or an interleukin 1 inhibitor. J. Immunol. **134:**3868–3875.
6. **Arend, W. P., M. Malyak, M. F. Smith, T. D. Whisenand, J. L. Slack, J. E. Sims, J. G. Giri, and S. K. Dower.** 1994. Binding of IL-1α, IL-1β, and IL-1 receptor antagonist by soluble IL-1 receptors and levels of soluble IL-1 receptors in synovial fluids. J. Immunol. **153:**4766–4774.
7. **Balavoine, J. F., B. de Rochemonteix, P. Seckinger, A. Cruchaud, and J. M. Dayer.** 1986. Prostanglandin E2 and collagenase production by fibroblasts and synovial cells is regulated by urine-derived human interleukin 1 and inhibitor(s). J. Clin. Investig. **78:**1120–1124.
8. **Bernardini, M. L., J. Mounier, H. d'Hauteville, M. Coquis-Rondon, and P. J. Sansonetti.** 1989. Identification of *icsA*, a plasmid locus of *Shigella flexneri* which governs bacterial intra- and intercellular spread through interaction with F-actin. Proc. Natl. Acad. Sci. USA **86:**3867–3871.
9. **Black, R. A., S. R. Kronheim, M. Cantrell, M. C. Deeley, C. J. March, J. Wignall, P. J. Conlon, D. Cosman, and T. P. Hopp.** 1988. Generation of biologically active interleukin-1 beta by proteolytic cleavage of the inactive precursor. J. Biol. Chem. **263:**9437–9442.
10. **Cannon, J. G., B. D. Clark, P. Wingfield, U. Schmeissner, C. Losberger, C. A. Dinarello, and A. R. Shaw.** 1989. Rabbit IL-1: cloning, expression, biologic properties, and transcription during endotoxemia. J. Immunol. **142:**2299–2306.
11. **Casini-Raggi, V., L. Kam, Y. J. T. Chong, C. Fiocchi, T. T. Pizarro, and F. Cominelli.** 1995. Mucosal imbalance of IL-1 and IL-1 receptor antagonist in inflammatory bowel disease. J. Immunol. **154:**2434–2440.
12. **Chen, Y., M. R. Smith, K. Thirumalai, and A. Zychlinsky.** 1996. A bacterial invasin induces macrophage apoptosis by binding directly to ICE. EMBO J. **15:**3853–3860.
13. **Cheney, C. P., S. B. Formal, P. A. Schad, and E. C. Boedecker.** 1983. Genetic transfer of a mucosal adherence factor (R1) from an enteropathogenic *Escherichia coli* strain into a *Shigella flexneri* strain and the phenotypic suppression of this adherence factor. J. Infect. Dis. **147:**711–723.
14. **Chomczynski, P., and N. Sacchi.** 1987. Single-step method of RNA isolation by acid guanidium thiocyanate-phenol-chloroform extraction. Anal. Biochem. **162:**156–159.
15. **Cominelli, F., C. C. Nast, A. Duchini, and M. Lee.** 1992. Recombinant interleukin-1 receptor antagonist blocks the proinflammatory activity of endogenous interleukin-1 in rabbit immune colitis. Gastroenterology **103:**65–71.
16. **Cominelli, F., C. C. Nast, B. D. Clark, R. Schindler, R. Llerena, V. E. Eysselein, R. C. Thompson, and C. A. Dinarello.** 1990. Interleukin-1 (IL-1) gene expression, synthesis, and effect of specific IL-1 receptor blockade in rabbit immune complex colitis. J. Clin. Investig. **86:**972–980.
17. **Dinarello, C. A.** 1996. Biologic basis for interleukin-1 in disease. Blood **87:**2095–2147.
18. **Dripps, D. J., B. J. Brandhuber, R. C. Thompson, and S. P. Eisenberg.** 1991. Interleukin (IL-1) receptor antagonist binds to the 80-kDa IL-1 receptor but does not initiate IL-1 signal transduction. J. Biol. Chem. **266:**10331–10336.
19. **Eisenberg, S. P., R. J. Evans, and W. P. Arend.** 1990. Primary structure and functional expression from complementary DNA of a human interleukin-1 receptor antagonist. Nature **343:**341–346.
20. **Fischer, E., K. J. Van Zee, M. A. Marano, C. S. Rock, J. S. Kenney, D. D. Poutsiaka, C. A. Dinarello, S. F. Lowry, and S. S. Moldawer.** 1992. Interleukin-1 receptor antagonist circulates in experimental inflammation and in human disease. Blood **79:**2196–2200.
21. **Furutani, Y., M. Notake, M. Yamayoshi, J. Y. Yamagishi, H. Nomura, M. Ohue, R. Furuta, T. Fukui, M. Yamada, and S. Nakamura.** 1985. Cloning and characterization of the cDNAs for human and rabbit interleukin-1 precursor. Nucleic Acids Res. **13:**5869–5881.
22. **Gavrieli, Y., Y. Sherman, and S. A. Ben-Sasson.** 1992. Identification of programmed cell death *in situ via* specific labeling of nuclear DNA fragmentation. J. Cell Biol. **119:**493–501.
23. **Goldberg, M., O. Barzu, C. Parsot, and P. J. Sansonetti.** 1993. Unipolar localization and ATPase activity of IcsA, a *Shigella flexneri* protein involved in intracellular movement. J. Bacteriol. **175:**2189–2196.
24. **Granowitz, E. V., A. Santos, D. D. Poutsiaka, J. G. Cannon, D. W. Wilmore, S. M. Wolff, and C. A. Dinarello.** 1991. Production of interleukin-1 receptor antagonist during experimental endotoxemia. Lancet **338:**1423–1424.
25. **Griffais, R., P. M. André, and M. Thibon.** 1991. K-tuple frequency in the human genome and polymerase chain reaction. Nucleic Acids Res. **19:**3887–3891.
26. **Gruss, H. J., G. Doelken, M. A. Brach, M. R. Mertelsman, and F. Herrmann.** 1992. High concentrations of the interleukin-1 receptor antagonist in serum of patients with Hodgkin's disease. Lancet **340:**968.
27. **Hale, T. L.** 1998. Bacillary dysentery, p. 479–493. *In* W. J. Hansler and M. Shuman (ed.), Topley & Wilson's microbiology and microbial infections, vol. 3. Arnold, London, England.
28. **Harris, D. E., D. M. Warshaw, and M. Periasamy.** 1992. Nucleotide sequences of the rabbit alpha-smooth-muscle and beta-non-muscle actin mRNAs. Gene **112:**265–266.
29. **Haskill, S., G. Martin, L. Van Le, J. Morris, A. Peace, C. F. Bigler, G. J. Jaffe, C. Hammerberg, S. A. Sporn, S. Fong, W. P. Arend, and P. Ralph.** 1991. cDNA cloning of an intracellular form of the human interleukin 1 receptor antagonist associated with epithelium. Proc. Natl. Acad. Sci. USA **88:**3681–3685.
30. **Heresbach, D., M. Alizadeh, and A. Dabadie.** 1997. Significance of interleukin-1 beta and interleukin-1 receptor antagonist genetic polymorphism in inflammatory bowel diseases. Am. J. Gastroenterol. **92:**1164–1169.
31. **Hilbi, H. J., E. Moss, D. Hersh, Y. Chen, J. Arondel, R. A. Banerjee, J. Flavell, J. Yuan, P. J. Sansonetti, and A. Zychlinsky.** 1998. *Shigella*-induced apoptosis is dependent on caspase-1 which binds to IpaB. J. Biol. Chem. **273:**32864.
32. **Inman, L. R., and J. R. Cantey.** 1984. Peyer's patch lymphoid follicle epithelial adherence of a rabbit enteropathogenic *Escherichia coli* (strain RDEC-1). Role of plasmid-mediated pili in initial adherence. J. Clin. Investig. **74:**90–95.
33. **Islam, D., B. Veress, P. K. Bardhan, A. A. Lindberg, and B. Christensson.** 1997. *In situ* characterization of inflammatory responses in the rectal mucosae of patients with shigellosis. Infect. Immun. **65:**739–749.
34. **Jung, H. C., L. Eckmann, S.-K. Yang, P. Asit, J. Fierer, E. Morzycka-Wroblewska, and M. Kagnoff.** 1995. A distinct array of proinflammatory cytokines is expressed in human colon epithelial cells in response to bacterial invasion. J. Clin. Investig. **95:**55–65.
35. **Kuhn, R., L. Lohler, D. Rennick, K. Rajewsky, and W. Muller.** 1993. Interleukin-10-deficient mice develop chronic enterocolitis. Cell **75:**263–274.
36. **Kuida, K., J. A. Lippke, G. Ku, M. W. Harding, D. J. Livingston, M. S.-S. Su, and R. A. Flavell.** 1995. Altered cytokine export and apoptosis in mice deficient in interleukin-1β converting enzyme. Science **267:**2000–2003.
37. **LaBrec, E. H., H. Schneider, T. J. Magnani, and S. B. Formal.** 1964. Epithelial cell penetration as an essential step in the pathogenesis of bacillary dysentery. J. Bacteriol. **88:**1503–1518.
38. **Li, P., H. Allen, S. Banerjee, S. Franklin, L. Herzog, C. Johnston, J. McDowell, M. Paskind, L. Rodman, J. Salfeld, E. Towne, D. Tracey, S. Wardwell, F.-Y. Wey, W. Wong, R. Kamen, and T. Seshadri.** 1995. Mice deficient in interleukin-1 converting enzyme (ICE) are defective in production of mature interleukin-1β and resistant to endotoxic shock. Cell **80:**401–411.
39. **Makino, S., C. Sasakawa, K. Kamata, T. Kurata, and M. Yoshikawa.** 1986. A genetic determinant required for continuous reinfection of adjacent cells on large plasmid in *S. flexneri* 2a. Cell **46:**551–555.
40. **Matsukawa, A., T. Fukumoto, T. Maeda, S. Ohkawara, and M. Yoshinaga.** 1997. Detection and characterization of IL-1 receptor antagonist in tissues from healthy rabbits: IL-1 receptor antagonist is probably involved in health. Cytokine **9:**307–315.
41. **Matsukawa, A., S. Ohkawa, T. Maeda, K. Akagi, and M. Yoshinaga.** 1993. Production of IL-1 and IL-1 receptor antagonist and the pathological significance in lipopolysaccharide-induced arthritis in rabbits. Clin. Exp. Immunol. **93:**206–211.
42. **Ménard, R., P. J. Sansonetti, and C. Parsot.** 1993. Nonpolar mutagenesis of the *ipa* genes defines IpaB, IpaC, and IpaD as effectors of *Shigella flexneri* entry into epithelial cells. J. Bacteriol. **175:**5899–5906.
43. **Ménard, R., P. J. Sansonetti, and C. Parsot.** 1994. The secretion of the *Shigella flexneri* Ipa invasins is induced by the epithelial cell and controlled by IpaB and IpaD. EMBO J. **13:**5293–5302.
44. **Ménard, R., P. J. Sansonetti, C. Parsot, and T. Vasselon.** 1994. Extracellular association and cytoplasmic partitioning of the IpaB and IpaC invasins of *Shigella flexneri*. Cell **79:**515–525.
45. **Miller, L. C., E. A. Lynch, S. Isa, J. W. Logan, C. A. Dinarello, and A. C. Steere.** 1993. Balance of synovial fluid IL-1β and IL-1 receptor antagonist and recovery from Lyme arthritis. Lancet **341:**146–148.
46. **Mounier, J., T. Vasselon, R. Hellio, M. Lesourd, and P. J. Sansonetti.** 1992. *Shigella flexneri* enters human colonic Caco-2 epithelial cells through their basolateral pole. Infect. Immun. **60:**237–248.

47. **Perdomo, J. J., J. M. Cavaillon, M. Huerre, H. Ohayon, P. Gounon, and P. J. Sansonetti.** 1994. Acute inflammation causes epithelial invasion and mucosal destruction in experimental shigellosis. J. Exp. Med. **180:**1307–1319.
48. **Perdomo, J. J., P. Gounon, and P. J. Sansonetti.** 1994. Polymorphonuclear leukocyte transmigration promotes invasion of colonic epithelial monolayer by *Shigella flexneri*. J. Clin. Investig. **93:**633–643.
49. **Phalipon, A., M. Kaufmann, P. Michetti, J. M. Cavaillon, M. Huerre, P. J. Sansonetti, and J. P. Kraehenbühl.** 1995. Monoclonal immunoglobulin A antibody directed against serotype-specific epitope of *Shigella flexneri* lipopolysaccharide protects against murine experimental shigellosis. J. Exp. Med. **182:**769–778.
50. **Rambaldi, A., M. Torcia, S. Bettoni, E. Vannier, T. Barbui, A. R. Shaw, C. A. Dinarello, and F. Cozzolino.** 1991. Modulation of cell proliferation and cytokine production in acute myeloblastic leukemia by interleukin-1 receptor antagonist and lack of its expression by leukemic cells. Blood **78:**3248–3253.
51. **Raqib, R., A. A. Lindberg, B. Wrething, P. K. Bardhan, U. Andersson, and J. Andersson.** 1995. Persistence of local cytokine production in shigellosis in acute and convalescent stages. Infect. Immun. **63:**289–296.
52. **Roussomoustakaki, M., J. Satsangi, and K. Welsh.** 1997. Genetic markers may predict disease behavior in patients with ulcerative colitis. Gastroenterology **112:**1845–1853.
52a. **Sansonetti, P. J., and J. Arondel.** Unpublished results.
53. **Sansonetti, P. J., and J. Arondel.** 1989. Construction and evaluation of a double mutant of *Shigella flexneri* as a candidate for oral vaccination against shigellosis. Vaccine **7:**443–450.
54. **Sansonetti, P. J., D. J. Kopecko, and S. B. Formal.** 1982. Involvement of a large plasmid in the invasive ability of *Shigella flexneri*. Infect. Immun. **35:**852–860.
55. **Sansonetti, P. J., J. Arondel, J. M. Cavaillon, and M. Huerre.** 1995. Role of IL-1 in the pathogenesis of experimental shigellosis. J. Clin. Investig. **96:**884–892.
56. **Sansonetti, P. J., J. Arondel, R. J. Cantey, M. C. Prévost, and M. Huerre.** 1996. Infection of rabbit Peyer's patches by *Shigella flexneri*: effect of adhesive or invasive bacterial phenotypes on follicule-associated epithelium. Infect. Immun. **64:**2752–2764.
57. **Sims, J. E., J. G. Giri, and S. K. Dower.** 1994. The two interleukin-1 receptors play different roles in IL-1 activities. Clin. Immunol. Immunopathol. **72:**9–14.
58. **Wakabayashi, G., J. A. Gelfand, W. K. Jung, R. J. Connolly, J. F. Burke, and C. A. Dinarello.** 1991. Staphylococcus epidermidis induces complement activation, tumor necrosis factor and interleukin-1, a shock-like state and tissue injury in rabbits without endotoxemia. J. Clin. Investig. **87:**1925–1935.
59. **Wassef, J., D. F. Keren, and J. L. Mailloux.** 1989. Role of M cells in initial bacterial uptake and in ulcer formation in the rabbit intestinal loop model in shigellosis. Infect. Immun. **57:**858–863.
60. **Watanabe, N., and Y. Kobayashi.** 1994. Selective release of a processed form of interleukin-1a. Cytokine **6:**597–601.
61. **Wilbur, W. J., and D. J. Lipman.** 1983. Rapid similarity searches of nucleic acid and protein data banks. Proc. Natl. Acad. Sci. USA **80:**726–730.
62. **Zychlinsky, A., and P. J. Sansonetti.** 1997. Host/pathogen interactions. Apoptosis in bacterial pathogenesis. J. Clin. Investig. **100:**493–496.
63. **Zychlinsky, A., and P. J. Sansonetti.** 1997. Apoptosis as a proinflammatory event: what can we learn from bacteria-induced cell death? Trends Microbiol. **5:**201–204.
64. **Zychlinsky, A., B. Kenny, R. Ménard, M. C. Prévost, I. B. Holland, and P. J. Sansonetti.** 1994. IpaB mediates macrophage apoptosis induced by *Shigella flexneri*. Mol. Microbiol. **11:**619–627.
65. **Zychlinsky, A., C. Fitting, J. M. Cavaillon, and P. J. Sansonetti.** 1994. Interleukin 1 is released by macrophages during apoptosis induced by *Shigella flexneri*. J. Clin. Investig. **94:**1328–1332.
66. **Zychlinsky, A., K. Thirumalai, J. Arondel, J. R. Cantey, A. O. Aliprantis, and P. J. Sansonetti.** 1996. In vivo apoptosis in *Shigella flexneri* infections. Infect. Immun. **64:**5357–5365.
67. **Zychlinsky, A., M. C. Prévost, and P. J. Sansonetti.** 1992. *Shigella flexneri* induces apoptosis in infected macrophages. Nature **358:**167–169.

Editor: J. R. McGhee